



# Reactive compatibilization of polycarbonate/polyester blends: optical and rheological properties

A AL-JABAREEN<sup>1,\*</sup>  and O O SANTANA<sup>2</sup>

<sup>1</sup>Materials Engineering Department, Al-Quds University, East Jerusalem 20002, Palestine

<sup>2</sup>Centre Català del Plàstic, Universitat Politècnica de Catalunya (UPC), Colom 114, 08222 Terrassa, Spain

\*Author for correspondence (ahmad.jabareen@staff.alquds.edu)

MS received 12 March 2023; accepted 14 September 2023

**Abstract.** Optical and rheological properties of polycarbonate (PC)/poly(ethylene terephthalate) (PET) blends rich in PC with the presence or absence of different types of transesterification catalysts were investigated in this study. PC/PET blends maintain a high level of transparency (transmittance between 86 and 93%) in all cases, regardless of the blending ratio or the presence or absence of transesterification catalysts. These variations in transmittance are due to the size, distribution and number of dispersed particles. The linear viscoelastic properties confirmed the partial miscibility of blends containing transesterification catalysts in the polymer melt. Additionally, the Palierne emulsion model, with a few changes, gave accurate predictions of the linear viscoelastic data for all PC/PET blends. However, as predicted, the low-frequency data demonstrated the distinct impact of interfacial tension on the elastic modulus of the blends, particularly, as the PET content is increased.

**Keywords.** Blends; compatibilization; rheology; transesterification.

## 1. Introduction

In some blends, such as poly(ethylene terephthalate) (PET)/polycarbonate (PC), the ester exchange reaction or transesterification is well established in polyesters at melt-processing temperatures above 240°C. Most of the previous studies have focused on the crystallization [1], morphology [2,3], compatibility [4,5], thermal properties [6–8] and mechanical properties [9,10] of these blends.

In our previous works [11, 12], we used the reactive extrusion method to study the mechanical, thermal, morphological and thermal properties of PET/PC blends rich in PC and in the presence or absence of different types of transesterification catalysts. It was reported that all blends were composed of a semi-crystalline (12–20% crystallinity) PET-dispersed phase and a PC matrix. When a transesterification catalyst was used in the reactive extrusion process, the PET phase was dispersed more precisely and uniformly, and the dynamic mechanical behaviour of PC/PET blends is improved compared to pure PC. This is supported by the tensile results, which show that the elastic modulus and yield stress are significantly larger for the blends with transesterification catalysts than for pure PC. The PET–PC copolymer produced during the transesterification reaction may have an emulsifying effect, which could explain this behaviour. The glass transition ( $T_g$ ) shift of the PC and PET phases

further demonstrates how this copolymer leads to the miscibility between the phases.

Study of the rheological behaviour of PET/PC composites receives less attention. One example is provided by Carrot [13], who made blends of 50/50 PET and PC and examined the impact of various catalysts on the morphology using rheological techniques. When the storage modulus at 0.25 rad s<sup>-1</sup>, was plotted against the composition, a distinctive pattern in the blends was observed when optimum elasticity is equal to one. This maximum is correlated with a region of phase inversion.

Nabar and Kale [14] compared the rheological properties of PET/PC and poly(butylene terephthalate) (PBT)/ PC blends. He found that the rheology of PC–PBT blends appears to exhibit regular fluctuation with mixing time. However, for PET/PC blends, the extruder's processing time and catalyst remaining in the commercial sample result in an adequate level of transesterification. The random copolymer formed shows significantly lower viscosity than PC, PET and PBT.

PET/PC extruded blends have been widely studied, especially in terms of the effect of the type and amount of catalyst used on their thermal, dynamic and mechanical properties [15–18]. However, very little information is available on the optical properties of PET/PC blends. For example, transparency, which is one of the most important characteristics of PET and PC, should be maintained during

the blending process in some cases, to meet special applications. The majority of PET/PC blends obtained, nevertheless, are opaque, making transparency impossible to maintain [19]. Moreover, although it is important to maintain transparency when improving other properties, there has been little discussion of the transparency and haze or optical properties of blends in general.

In addition, studies on their polymer melt properties are scarce. Considering relaxation time as an example, the viscosity to modulus at zero shear, determines both the relaxation of orders during mould filling and also in controlling the solidification process. To the best of our knowledge, no work has yet been published focusing on melt properties like the time of relaxation, as here, in our work.

The objectives of this work are the following: to identify the proper applications for the material and polymer processing, such as extrusion and injection moulding, it is necessary first to study the rheological behaviour of PC/PET blends and secondly, to investigate how the degree of transparency or the optical behaviour changes in these blends. In total, this study will cover a special behaviour of these blends where the lack of studies was found and hence, a complete study will be done about these blends.

## 2. Experimental

### 2.1 Material preparation and blending

The materials and procedures used for the PC/PET blend preparations were reported in previous papers [11,12] and will be discussed very briefly. A melt mixture of PET copolymer ( $IV = 0.80 \text{ dl g}^{-1}$ ) and Lexan 123R PC (MFI = 10 g per 10 min) was produced using a COLLIN ZK-25 co-rotating twin screw extruder at 190–270°C and 130–160 rpm. The added PET contents were 10, 20 and 30% by weight, and the following code will be applied: PC## with ## denoting the average PC content (PC90, PC80 and PC70). A catalyst (if used) is first manually mixed into polymer pellets at a concentration of 0.05 mass% with respect to the final products. The catalysts used were zinc acetate hydrate ( $\text{Zn}(\text{CH}_3\text{COO})_2 \cdot 2\text{H}_2\text{O}$ ), calcium acetate hydrate ( $\text{Ca}(\text{CH}_3\text{COO})_2 \cdot x\text{H}_2\text{O}$ ), Samarium acetyl acetonate ( $\text{Sm}(\text{acac})_3 \cdot x\text{H}_2\text{O}$  ( $x = 3-4$ )), all of which were obtained from Aldrich.

Under the same processing conditions of the melt-blending process, the extrudates were extruded once more by a Collin Teach Line 20T-E single screw extruder to obtain 0.7 mm sheets. The raw materials were dried before melt blending. Polymers were maintained at 120°C for 4 h in a PIOVAN T30IX dehumidifying dryer hopper.

### 2.2 Measurements

The transmittance values from the solid-state UV–Vis spectra obtained with an HP 845X UV–Vis spectrometer

using Izod bars and Gardner disks were used to compute the yellowness index (YI). As a result, the following relationship [20] was used to determine YI:

$$YI = \frac{T_{680} - T_{420}}{T_{560}}, \quad (1)$$

where  $T$  is the transmittance at the given wavelength.

According to ASTM-1003/290, haze tests were conducted using a HazeGard (BYK-Gardner) haze meter. Haze is that part of the transmitted light that deviates from the average direction of the incident light beam by  $>2.5^\circ$ .

Using air as a reference material (100% transmittance), a Perkin-Elmer Lambda 900 photometer was used to determine the transmittance. According to the method E 308 (ASTM D 1003-61), transmittance is the percentage of transmission compared to incident light.

The dynamic properties of the polymers were measured using a rheometric mechanical spectrometer (AR-G2), and the outcomes were analysed using the rheology advanced data analysis program (ver. V.5.4.8). Parallel-plate geometry was used to evaluate the rheological properties. The bottom disk was fixed, while the upper disk oscillated at an angular velocity ( $\omega$ ). The diameter of the parallel plate was 25 mm and the distance between them was 0.6 mm. The top plate was rotated during testing in a small-amplitude (strain between 3 and 10% or 900 Pa stress) sinusoidal oscillation at an angular frequency sweep between 0.1 and 200  $\text{rad s}^{-1}$  at 260°C. Before performing the dynamic tests, all samples were dried for a minimum of 4 h at 120°C. To avoid degradation, the tests were carried out in a nitrogen atmosphere.

To conduct the dynamic test, first, it was necessary to ensure that the substance would not degrade, while it was being tested. Time sweep experiments were carried out to make sure that there is no degradation. These experiments measure dynamic properties, such as complex viscosity as a function of time at a fixed frequency and strain. A strain sweep test was run at a fixed frequency to determine the linear region of the dynamic properties. All materials exhibited linear behaviour at strain values between 3 and 10%.

## 3. Results and discussion

### 3.1 Colour and transparency analyses

Table 1 presents the optical properties of neat polymers and PC/PET sheet samples. Neat PC exhibits good transparency due to the amorphous nature of polycarbonate. Similarly, neat PET shows a transparent appearance. This means that the PET copolymer used is amorphous or has a low crystallinity ( $<4\%$  [12]), but it is still more opaque than PC polymer. The amorphous state of PET is due to the cooling conditions employed on the sheet sample during the calendering process. The transparency observed in the test

**Table 1.** Optical properties of neat polymers and PC/PET blends.

Material	Haze (%)	Transmittance (%)	Yellow index (ANSI)
PC	2.8	93.1	1.5
PC90	22.9	91.1	1.6
PC90Ca	27.5	88.9	3.6
PC90Zn	15.1	91.2	10.5
PC90Sm	30.6	87.1	15.4
PC80	34.9	90.0	0.7
PC80Ca	34.1	88.2	3.5
PC80Zn	28.1	88.2	7.1
PC80Sm	35.4	86.4	17.2
PC70	35.7	89.1	0.9
PC70Zn	32.3	86.4	5.7
PET	3.6	91.4	2.0

specimen of pure PET indicates that despite its crystallinity, the morphology of the crystalline phase does not generate significant light scattering processes, which cause opacity of the specimen.

Increasing PET content promotes a gradual optical change from transparent to opaque. Measurements conducted by exploratory optical properties in the sheet determined that the fraction of light transmitted is reduced from 93.1 to 89.1% when it moves from 0 to 30% by weight PET.

According to transmittance values and compared with neat polymers, the transparency of PC/PET blends with transesterification catalysts is decreased due to some interchange reaction occurring in that system, as seen by FTIR analysis [12].

As a result of this reaction, three different phases were found together in the same blend system: the amorphous phase, which represents PC segments, the PET copolymer phase (crystalline one) that did not react during the blending process and the copolymer product that was generated during the transesterification reaction. Each phase has its own density, therefore, its own refractive index, which reduces the transmittance of the light that passes through the specimen sheet.

In the opposite way, the haze of the sheet specimen of neat PET is more than that of PC. This is associated with the semicrystalline segments that were found in the PET. The haze values increase from 2.8% for a neat PC specimen (0% PET) to 35.7% for the PC70 specimen (30% PET). The opacity observed here is not related to the crystallization process, but rather to the existence of at least two or three phases in the solid state with different densities, and the dispersion and size of particles. By increasing the amount of PET, the blend dispersion becomes less fine and the particle size increases [12].

Generally, in the case of PC/PET blends in the presence of transesterification catalysts, the copolymer which forms during melt blending acts as a compatibilizing or emulsifying agent that makes a fine dispersion of the phases and therefore, enhances the optical properties [12].

This can be seen by comparing the haze values of blends that were prepared with catalysts with those which do not have catalysts. One can observe that blends prepared with the Zn-based catalyst, exhibit the lowest haze values compared with other catalysed systems, which is a consequence of the fine dispersion morphology of these blends [12].

The specimen sheet of neat PC exhibits a yellow index value of 1.48 compared with a higher value of 2.04 for the neat PET specimen sheet. The addition of PET decreased the yellow index value to about 0.96 in the case of PC70.

The presence of base catalysts like Zn, Sm and Ca is capable of promoting interchange reactions between PET and PC phases. Initially, these catalysts also encourage the degradation reaction of PET. This leads to the formation of terminal carboxyl groups, which then suffer from acidic reactions and form terminal  $-OCOOH$  group segments of the PC. The latter is involved in a decarboxylation side reaction that releases  $CO_2$  and forms terminal phenol groups, which give the yellow color [21].

PC/PET blends with Zn-based catalyst appear yellow, the colour of the catalyst used. It seems that the intensity of the yellow colour is decreased by increasing the amount of PET in the system. Therefore, the yellow indices are 10.48 for PC90Zn, 7.10 for PC80Zn and 5.73 for PC70Zn.

Blends that contain the Sm-based catalyst have an orange colour, the colour of the Sm-based catalyst. Also, they have the highest yellow index values among the studied materials: 17.20 and 15.40 for PC90Sm and PC80Sm, respectively.

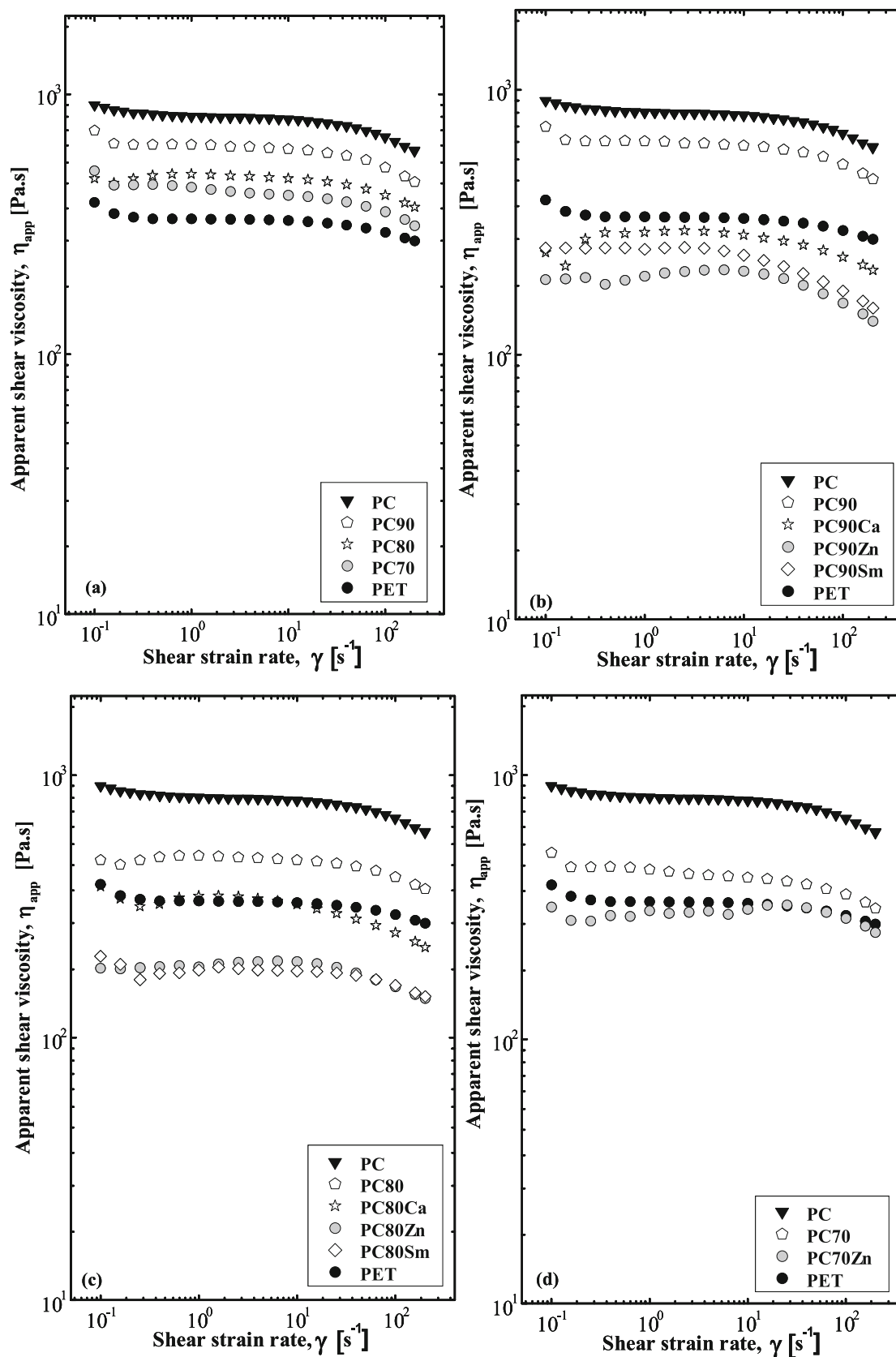
### 3.2 Rheological properties

Figure 1 shows the flow curves obtained at 260°C, in terms of apparent shear viscosity ( $\eta_{app}$ ) vs. shear strain rate ( $\dot{\gamma}$ ), after Cox–Merz transformation (i.e.,  $\eta(\dot{\gamma}) = |\eta^*(\omega)|\omega = \dot{\gamma}$ ) [22]. As observed, the parent polymers (PC and PET) have a wide strain rate range of Newtonian behaviour with the highest viscosity for PC. All blends without catalysts showed the same behaviour.

The addition of catalysts to PC90 and PC80 blends (figure 1b and c, respectively) clearly decreases the viscosity (even below that of PET) and the strain rate range, where Newtonian behaviour is observed (an increase of shear-thinning behaviour).

These observations imply that some degradation has occurred due to ester exchange reactions promoted by the catalyst. Although these reactions result in the production of PET–PC copolymers, they also cause significant chain splitting [13].

The relative decrease in melt-blend viscosity by the addition of a catalyst is higher as the PET content decreases. Hence, the hypothesis regarding the effect of dilution still emerges as the amount of catalyst has been kept constant in all the prepared blends.



**Figure 1.** Cox–Merz apparent shear viscosity ( $\eta_{app}$ ) vs. shear strain rate ( $\dot{\gamma}$ ) at 260°C for neat polymers: (a) blends without transesterification catalysts, and blends with transesterification catalysts: (b) PC90, (c) PC80 and (d) PC70.

Considering the changes in viscosity obtained, the Ca-based catalyst is the least active in terms of structural change, while the Zn-based catalyst, at least for the lowest amount of PET, is the most active. This contrasts with what has been reported in the literature, where the Sm-based catalyst tends to be the most active in this kind of reaction [23–25]. One must keep in mind that such modifications are a consequence of either transesterification or degradation processes.

Figure 2 shows the variation in the reduced dynamic modulus ( $G^*/G_N$ ) with the loss angle ( $\delta$ ) of the neat polymers and PC/PET blends. Since the plateau modulus can hardly be achieved in our experiments, the reduced modulus was determined by dividing the dynamic modulus ( $G^*$ ) by the value at the highest frequency ( $G_N$ ), i.e.,  $100 \text{ rad s}^{-1}$ . The van Gurp–Palmen plots [26] for homogeneous systems are depicted in figure 2, which is typically used to identify branching in polymers [27,28]. It has been suggested that it is also possible to use a van Gurp–Palmen plot to obtain indirect information on the morphology of immiscible or partially miscible polymer blends because it reflects the occurrence of a tail of long relaxation, which is linked to the presence of non-homogeneous domains.

van Gurp–Palmen plots of pure PC and PET show a conventional shape that is typically anticipated for linear polymers, with a plateau of the phase angle at  $90^\circ$  in the low angular frequency zone, suggesting nearly viscous behaviour. The phase angle diminishes as the angular frequency or modulus increases. Such typical plots for linear polyethylenes have been reported by Trinkle and Friedrich [27] and Fleury *et al.* [28]. These authors found that neither the average molecular weight nor the polydispersity affects the shape of these plots. Additionally, the curves only rely slightly on the chemical nature, and the curvature of the plot should be steeper when the polydispersity declines. Comparing the polydispersity degree (PD) between the neat polymers, it seems that PC has higher molecular weight distribution (MWD) due to the high flowability of that commercial polymer. All blends without catalyst showed similar trends at high frequencies, which means that PC/PET blend behaviour is independent of PET content.

For lower frequencies, a lower loss angle plateau ( $\delta$ ) is observed, depending on PET content, that tends to define a clear local minimum and maximum (even at lower  $\delta$ ) for PC70 blends (figure 2a). This lower plateau shows an overall improvement in elasticity compared to neat components. This behaviour is frequently seen for matrix/droplet morphogenesis; it corresponds to low-frequency relaxation and is explained by the effects of the interface [13]. The observed increase in  $\delta$  as PET content decreases, indicates a higher degree of homogeneity in the blends, even the existence of droplet morphology. This situation is expected, considering the morphological evidence obtained [12].

The use of the transesterification catalyst in the blends tends to increase the  $\delta$ , where plateau or local maximum is

observed, indicating that blend morphology is becoming more homogeneous, i.e., lower droplet size and/or better distribution of the dispersed phase.

Additionally, this change defines a steeper curvature compared to PC (matrix in blends), reflecting that the PD is decreased. This effect is greater for PC80Ca- and Sm-based catalysts (figure 2c). This behaviour is interpreted as a competition between the transesterification and degradation effects for this PET content.

Figure 3 shows the variation in  $G'$  with angular frequency ( $\omega$ ) for all blends at  $260^\circ\text{C}$ . By analysing it in detail, blends without transesterification catalysts present the expected behavior, i.e., the values of their respective  $G'$  are in between that of the parent polymers when  $\omega$  is above  $10 \text{ rad s}^{-1}$ .

For the blend compositions with lower contents of PET, the addition of a transesterification catalyst clearly diminishes this parameter to similar levels or even to levels lower than those observed for neat PET, and a negative deviation from the additive rule of mixtures is exhibited. This fact confirms what we mentioned earlier about a major modification of the chemical structure of the PC polymer matrix with a large component, is attributed to the degradation process.

It is worth noting that the decrease in this parameter is higher as the content of PET decreases. Note the little change that is seen for blends with 30 wt% of PET in the presence of Zn-based catalyst (figure 3d).

This effect is related to the morphological characteristics obtained, and it has been widely observed in emulsions, suspensions, the dispersion of inorganic additives in polymer matrices and immiscible polymer blends in which one of the phases shows a dispersion of the minor component. The deformability of droplets of the dispersed phase during the applied load has also been linked to an excess of elasticity or the incidence of secondary molecular relaxation with times of pronounced relation (longer relaxation times) [29–35]. The relaxation process slows down as the content of the dispersed phase rises due to the growth in the size of the droplets raising  $G'$  (figure 3a).

Figures 4–7 show the weighed relaxation spectrums of neat polymers, polymer blends without transesterification catalysts and blends with transesterification catalysts. For the estimation, a time range equivalent to the reciprocal of the frequency plus  $\exp(\pi/2)$  and 40 points per decade, were used. In this time range, there is greater certainty in the estimation [36]. It appears that blends show two well-defined relaxation regions that can be characterized by the relaxation time ( $\tau$ ) of the local maximum of the respective weighed spectrum ( $\tau \times H(\tau)$ ). The values obtained in this way are presented in table 2.

Addition of a transesterification catalyst clearly modifies these  $\tau$  values in PC90 and PC80 blends. In general, one can see an evident increase in those times in the presence of a transesterification catalyst. This seems to be more marked in the case of Sm-based catalyst, which would coincide with

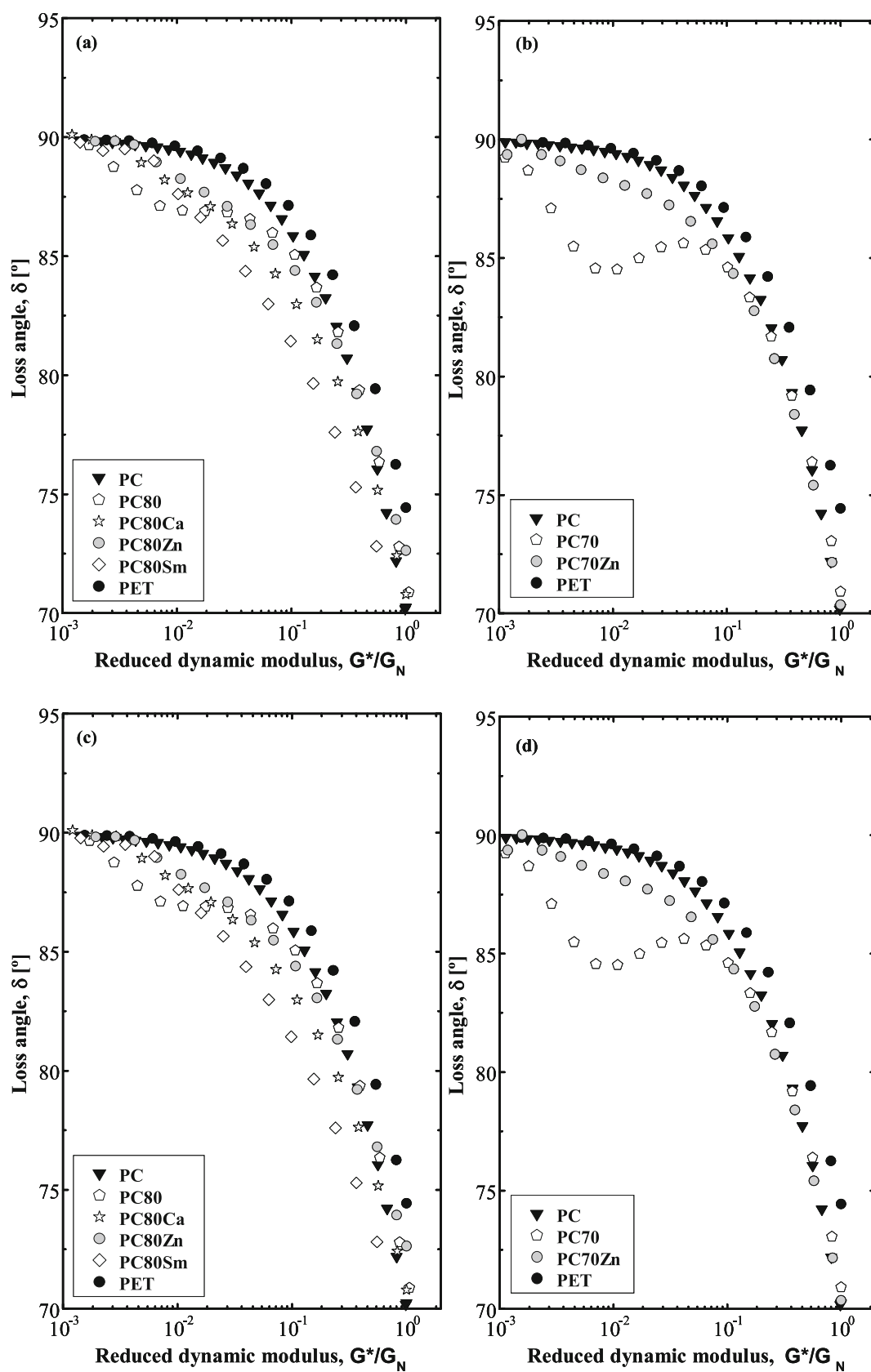


**Figure 2.** van Gurp–Palmen plots at 260°C for neat polymers: (a) blends without transesterification catalysts and blends with transesterification catalysts of (b) PC90, (c) PC80 and (d) PC70.

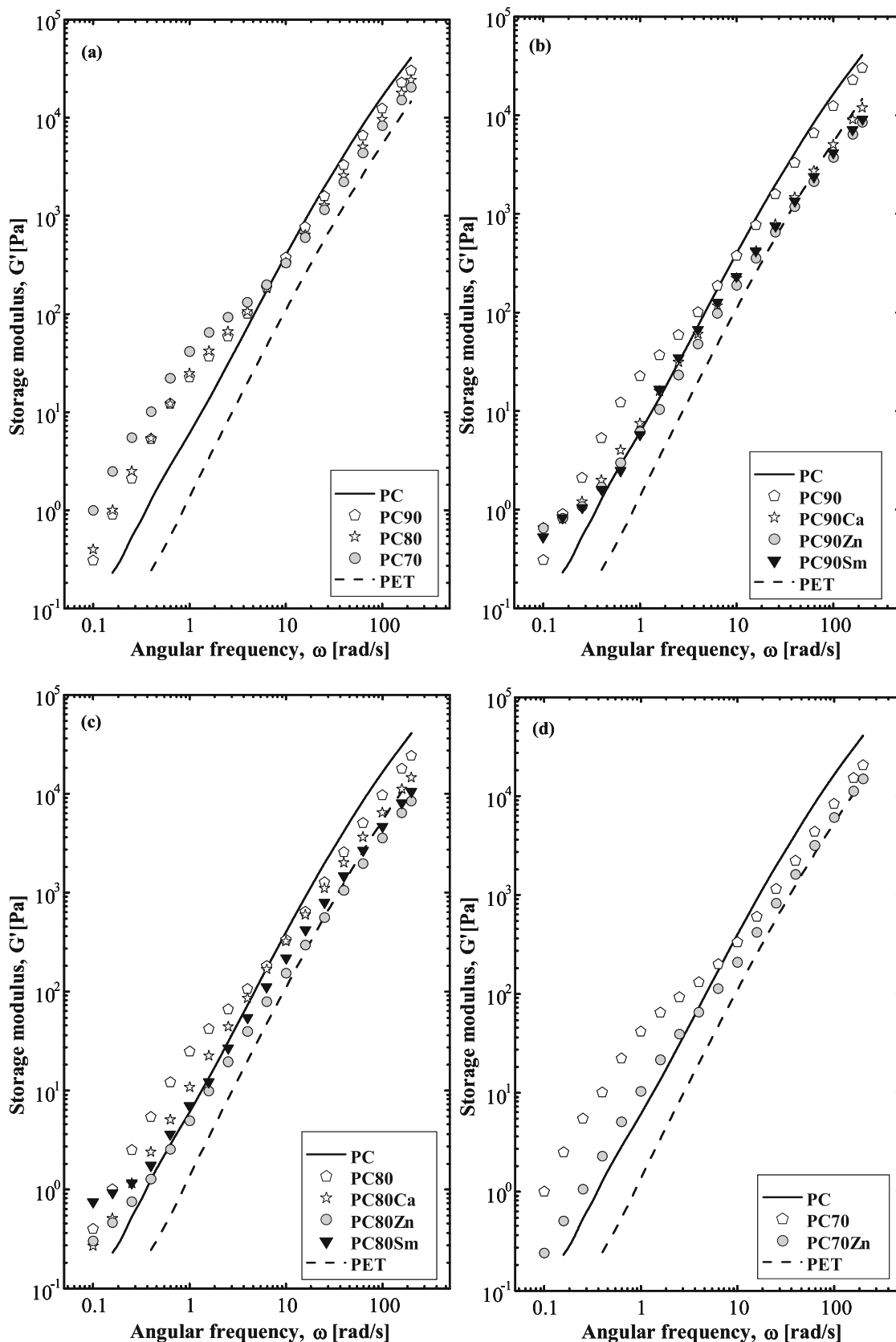


**Figure 3.** Variation in storage modulus ( $G'$ ) with the angular frequency ( $\omega$ ) of neat polymers: (a) blends with transesterification catalysts and blends with transesterification catalysts of (b) PC90, (c) PC80 and (d) PC70.

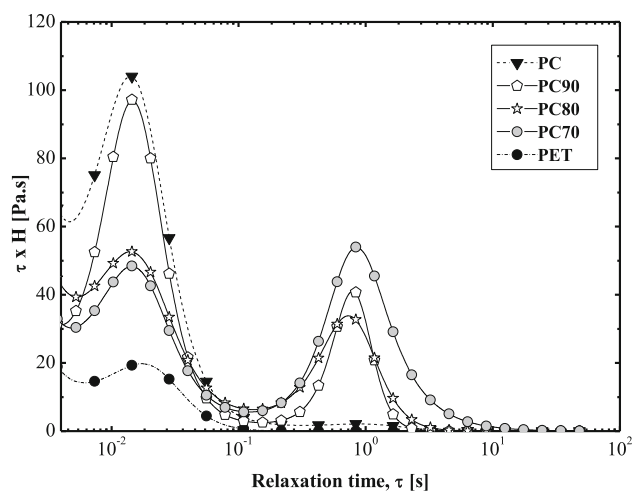


**Figure 4.** Weighed relaxation spectrum at 260°C for neat polymers and blends without transesterification catalysts.

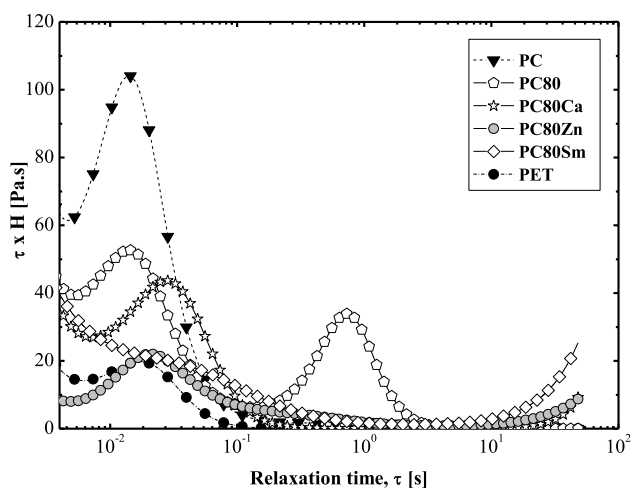


**Figure 6.** Weighed relaxation spectrum at 260°C for neat polymers and PC80 blends.

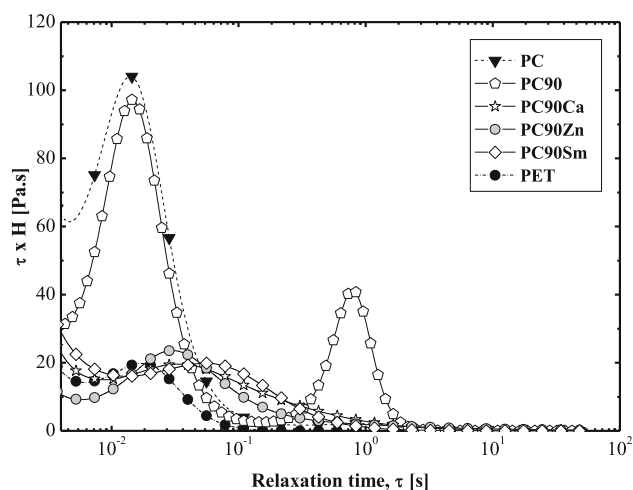


**Figure 5.** Weighed relaxation spectrum at 260°C for neat polymers and PC90 blends.

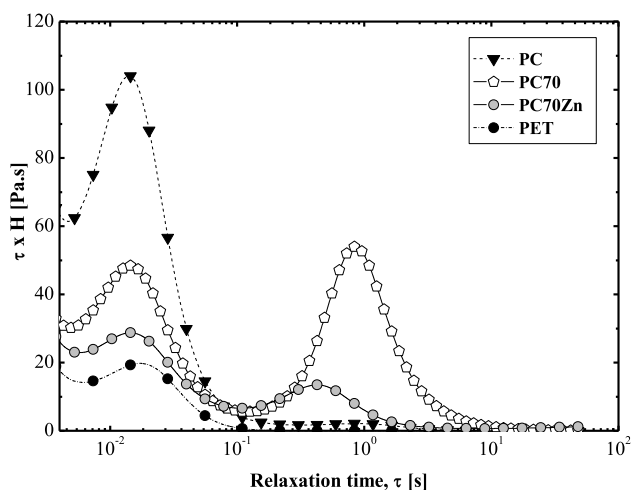


**Figure 7.** Weighed relaxation spectrum at 260°C for neat polymers and PC70 blends.

an increase in shear viscosity in the range of pseudoplastic behaviour of the material. This results from a greater proportion of side reactions leading to the degradation process. On the other hand, all the spectra curves for blends with transesterification catalysts have a single peak, which implies the miscibility or at least partial miscibility of blend components.

For blends without transesterification catalysts, and a second region at the highest  $\tau$  is observed with a well-defined local maximum located at  $\tau_1$  (figure 4 and table 2). This behaviour is associated with relaxation of the shape of the droplets during their deformation. One can see that although the maximum of the signal shows virtually no change with the PET content (dispersed phase), the width of the signal increases and spreads to the regions with the highest  $\tau$  values. This fact can be explained by keeping in

mind that an equilibrium between two forces determines the relaxation time of a droplet's shape [32,37]:

- A shear force that is proportional to the strain rate multiplied by the product of the strain rate tends to deform the particles in the dispersed phase.
- Cohesive force is proportional to the interfacial tension between the two phases ( $\alpha$ ) and its diameter ( $d$ ), which is related to the delay of the dispersed phase's ability to regain its spherical form (original shape).

As the dispersed phase's concentration rises, its diameter increases, as demonstrated by SEM in previous research [12]. This causes the proportional component of interfacial tension to decline and subsequently, it increases.

The fact that the position of the corresponding local maximum in the relaxation spectrum does not show

**Table 2.** Relaxation time ( $\tau$ ) is where there are local maxima in the weighed relaxation spectra at 260°C. The mean relaxation time,  $\tau_1$ , of the shape of the droplets was estimated by Palierne's model.

Material	$\tau \times 10^{-1}$ (s)	$\tau_1 \times 10^{-1}$ (s)
PC	1.45	—
PC90	1.45	7.80
PC90Ca	3.49	n.d.
PC90Zn	3.05	n.d.
PC90Sm	5.60	n.d.
PC80	1.45	7.29
PC80Ca	2.85	n.d.
PC80Zn	2.03	n.d.
PC80Sm	5.23	n.d.
PC70	1.45	8.35
PC70Zn	1.55	4.55
PET	1.78	—

significant variations, which indicate the compensation of this effect by a decrease in the viscosity of the phases as a result of transesterification reactions between them, in addition to the decrease in molecular weight (degradation).

The appearance of this  $\tau_1$  in emulsions and suspensions has served basically for the development of a viscoelastic model, where the dynamic response of the blends with their morphology, composition and the interfacial tension between its components are related. Among those models, the one proposed by Palierne and group [37], which is based on the ideas proposed by Choi and Showalter [38] for emulsions of Newtonian fluids.

Palierne and group [37] claim that the following abbreviated formula for the complex shear modulus ( $G_b^*$ ) of the blend, which is obtained if the interfacial tension between the matrix and the spherical dispersed phase is assumed to be independent of local shear and variation in the interfacial area:

$$G_b^*(\omega) = G_m^*(\omega) \frac{1 + 3 \sum_i \varphi_i H_i(\omega)}{1 - 2 \sum_i \varphi_i H_i(\omega)}, \quad (2)$$

with

$$H_i(\omega) = \frac{4 \left( \frac{\alpha}{R_i} \right) [2G_m^*(\omega) + 5G_i^*(\omega)] + [G_i^*(\omega) - G_m^*(\omega)] [16G_m^*(\omega) + 19G_i^*(\omega)]}{40 \left( \frac{\alpha}{R_i} \right) [G_m^*(\omega) + G_i^*(\omega)] + [2G_i^*(\omega) + 3G_m^*(\omega)] [16G_m^*(\omega) + 19G_i^*(\omega)]},$$

where  $\varphi_i$  is the volume proportion of inclusions with a radius of  $R_i$ ,  $\alpha$  the interfacial tension and  $G_i^*(\omega)$  and  $G_m^*(\omega)$  are the complex moduli of the dispersed phase and

matrix at the angular frequency ( $\omega$ ), respectively. For monodisperse morphologies, equation (2) could be simplified to equation (3):

$$G_b^*(\omega) = G_m^*(\omega) \frac{[1 + 3\varphi_i H_i(\omega)]}{[1 - 2\varphi_i H_i(\omega)]}, \quad (3)$$

assuming that  $R_i$  in equation (2) represents the volume average particle radius ( $R_n$ ).

Equation (2) can be used to calculate the interfacial tension as the value of  $\alpha$  that best fits the experimental data and the preceding equation. Since the ratio of  $\alpha/R$  is calculated, the accuracy of this estimation is then directly linked to the morphology. Likewise, it is possible to calculate the droplet's relaxation time by equation (4):

$$\tau_d = \frac{R_v \eta_m [19K + 16][2K + 3 - 2\varphi(K - 1)]}{4\alpha [10(K + 1) - 2\varphi(5K + 2)]}, \quad (4)$$

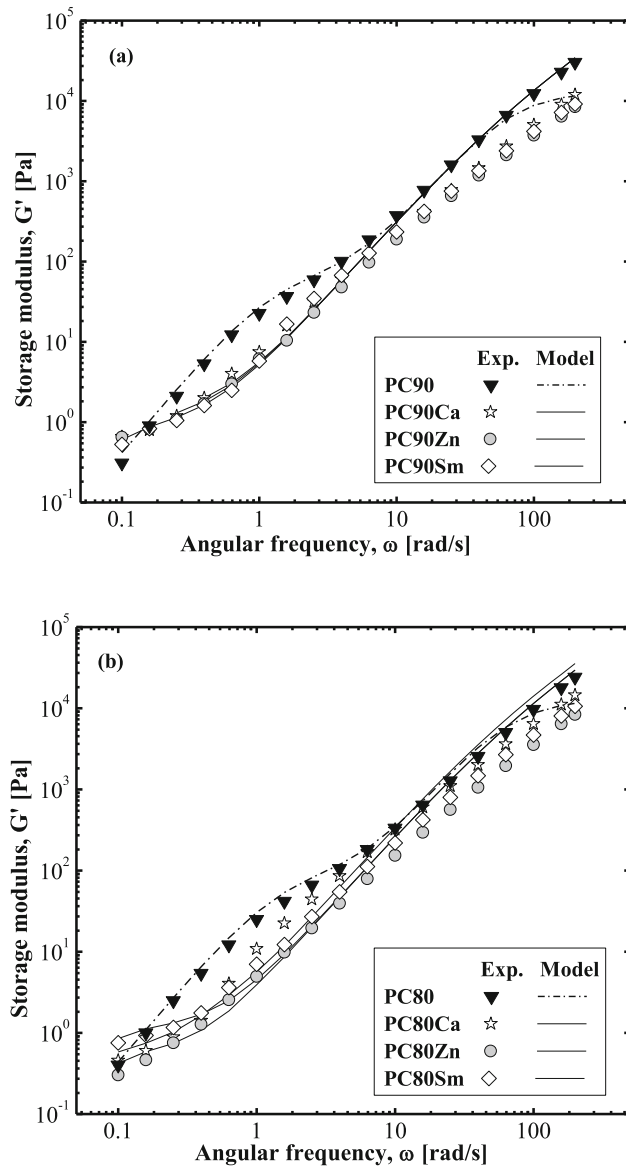
with  $K$  being the ratio of the parent polymers' viscosities (i.e.,  $\eta_m/\eta$ ) and  $\eta_m$  being the blend's matrix phase's Newtonian viscosity. Since both the polymers (PC and PET) showed close to Newtonian behaviour, equation (4) could be used.

Figure 8 shows the fitting between the experimental values of the  $G'$  vs.  $\omega$  and those made according to the model. As can be seen, the fitting is quite good in the range of low-angular frequency ( $\omega < 10 \text{ rad s}^{-1}$ ), mostly for PC90 and PC80 blends with transesterification catalysts. Some deviations are observed, mainly in blends without transesterification catalysts, as the PET content increases in PC80–PC70 and in PC70Zn.

This deviation is related to their morphological situations. According to Bousmina and Muller [39], in the case of concentrated blends (>15% of dispersed phase), the morphological situation seems to be like a network connecting the dispersed particles and aggregates, a situation that is not taken into account in emulsion models (Palierne's). This situation could imply a lower experimental value in the secondary plateau region than predicted by the model, as the emulsion model just considers the hydrodynamic interactions with no possibility of aggregation.

As can be seen in figure 9, the PC70Zn prediction shows the highest deviation. In this case, the actual geometry

observed i.e., filaments must be considered [12]. During the shearing, this morphology tends to describe a 'laminar' structure, giving rise to another kind of relaxation process



**Figure 8.** Experimental and Palierne's model predicted  $G'$  vs.  $\omega$  curves for (a) PC90 and (b) PC80 blends.

with different mechanisms involved, approaching a real co-continuous network with a higher relaxation time. Hence, the model is expected to fail.

Another deviation is observed at higher angular frequency ( $\omega > 10 \text{ rad s}^{-1}$ ). In the case of blends without transesterification catalysts, the model predicts an earlier deviation of  $G'$  at about  $40 \text{ rad s}^{-1}$ . Palierne's model considers that the terminal behaviour of the blends could be estimated as being the same of the matrix ( $G'_m$ ) modified by some function,  $g$  dependent on  $\phi$ ,  $K$  and the ratio of relaxation time of the matrix to the dispersed phase ( $\chi$ ). In this case, the relaxation time of the matrix and dispersed phase are estimated using a single Maxwell model (single relaxation time). It is well known that this

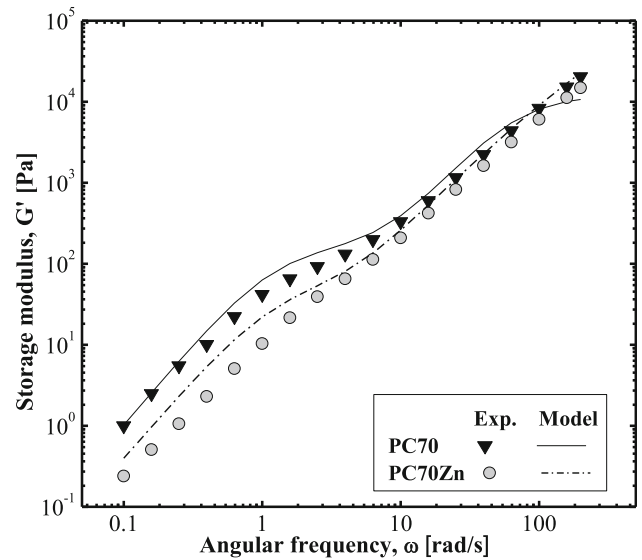


**Figure 9.** Experimental and Palierne's model predicted  $G'$  vs.  $\omega$  curves for PC70 blends.

consideration is unrealistic and yields the deviation observed at higher  $\omega$ .

In view of this systematic deviation, it seems more adequate to use for this region, a simple additive mixing rule (in its lower limit expression, 1-L or series mixing rule, equation 5) considering the experimental  $G'$  vs.  $\omega$  traces obtained for neat polymers in combination with low  $\omega$  Palierne's equation.

A similar procedure has been used by Jeon *et al.* [40] in polybutadiene/polyisoprene blends, but considering the higher limit expression (h-L) or a parallel mixing rule (equation 6).

$$G'_{1-L} = \left[ \frac{\phi_m}{G'_m} + \frac{\phi_d}{G'_d} \right], \quad (\text{Series}) \quad (5)$$

$$G''_{h-L} = \phi_m G''_m + \phi_d G''_d. \quad (\text{Parallel}) \quad (6)$$

It must be pointed out that in an attempt to reflect the morphology situation of emulsions of viscoelastic liquids, Coran and Patel [41] proposed a micromechanical model using both the above expressions by a weighed addition, in its  $G^*$  expression, is as follows:

$$G^*_{\text{blend}} = f \cdot G^*_{h-L} + [1 - f] G^*_{1-L}, \quad (7)$$

where the parameter  $f$  represents the parallel model's degree of applicability and provides a measurement for the phase's continuity with the maximum modulus value.

Even with this adjustment, a deviation still appears. It is even higher for the systems (PC90 and PC80) in the presence of transesterification catalysts, where the model predicts a higher  $G'$  value. However, fitting is quite good for

**Table 3.** Interfacial tension to mean radius ratio ( $\alpha/R$ ) at 260°C used as the fitting parameter in Palierne's model. Values were estimated for interfacial tension ( $\alpha$ ) and theoretical droplet relaxation time ( $\tau_d$ ) and experimental ( $\tau_1$ ), which are included for comparison proposes.

Material	$\alpha/R$ (N m <sup>-2</sup> )	$\alpha$ (mN m <sup>-2</sup> )	$\tau_d \times 10^{-1}$ (s)	$\tau_1 \times 10^{-1}$ (s)
PC90	1800	2.14	7.92	7.80
PC90Ca	110	0.16	127.0	n.d.
PC90Zn	80	0.22	174.6	n.d.
PC90Sm	90	0.17	174.6	n.d.
PC80	2100	2.21	7.49	7.29
PC80Ca	60	0.093	257.0	n.d.
PC80Zn	50	0.079	308.4	n.d.
PC80Sm	70	0.15	220.3	n.d.
PC70	1900	2.24	8.45	8.35
PC70Zn	2100	1.45	8.12	4.55

blends in this region without transesterification catalysts, indicating the following:

- Blends without transesterification catalyst show a linear viscoelastic behaviour following the mixing rule.
- Deviation observed in blends with transesterification catalysts should be attributed to side reactions, mostly chain splitting, promoted by the transesterification catalyst. However, the model fits quite well at low  $\omega$ , which is the region where elastic effects and interfacial tension between phases are clearly observed.

The fitting parameter (i.e.,  $\alpha/R$  ratio) and the estimated relaxation time of the dispersed phase ( $\tau_d$ ) are shown in table 3. Values of  $\alpha$  were estimated by taking the average volume and average radius of droplets obtained by SEM analysis [12]. Values obtained for blends without transesterification catalysts show an independence of the PET amount added and almost the same value (2.2 mN m<sup>-1</sup>) reported by Guerrica-Echevarría *et al.* [42] using the contact angle technique. The composition of independency should be expected from their partially miscible nature.

The use of transesterification catalysts in blend preparations causes a dramatic decrease in  $\alpha$ , a situation that should be expected considering the generation of PC-PET copolymer as one of the transesterification products. This result confirms the emulsifying action of this copolymer. A brief view of the results suggests that lower values are obtained as the PET amount increases when a spherical dispersed morphology is obtained. An actual trend in the effects of the type of transesterification catalyst used could not be made as the secondary plateau shifts to lower  $\omega$ , close to the precision limits of the device.

In the case of the PC70Zn blend, this should be considered doubtful due to the high concentration of the dispersed phase and the orientation effect on the morphology induced during the processing stage [12].

On the other side, there seems to be discrepancies between the estimated  $\tau_d$  and that obtained experimentally,

especially, in the case of PC90 blends in the presence of transesterification catalysts. According to Palierne's prediction, the weighed relaxation spectrum for this blend system (figure 5) should give a peak over 10–20 s that is not observed or detected.

In this case, one must consider the substantial modification suffered in matrix relaxation time not only in the peak value (shifting to higher times), but also in the relative height due to a high extent of structural or molecular weight modifications suffered. This is a situation that is clearly observed considering the higher  $\tau_d$  drop in viscosity observed for these blends. Also, considering the proportionality between the main and the secondary relaxation times provides a reason for a non-detected signal in the experimental spectrum, besides the doubtful region for its determination [36].

#### 4. Conclusion

The higher activity of the Sm-based catalyst than the other transesterification catalysts used, has been confirmed. However, at the same time, higher degradation effects were observed for this catalyst. Evidence of this phenomenon was obtained from the dynamic rheological (RDA) measurements, which showed a drastic decrease in low strain rate viscosities of the blends beyond those of the parent polymers. Also, as the PET content decreases, this effect is magnified if a comparison is made with the blends that do not have transesterification catalysts.

All PC/PET blends were partially miscible according to the weighed relaxation spectra and the log-additivity law for complex viscosity and the miscibility was enhanced by the presence of transesterification catalysts.

The sensitivity of the Palierne model predictions was tested considering  $\alpha/R$  (the ratio of interfacial tension and the average radius of the dispersed phase) as one parameter. For all the blends under consideration, the Palierne model predictions and the experimental results agree fairly well.

## Acknowledgement

Al-Jabareen, one of the authors, gratefully recognizes the PhD scholarship offered by the Ministerio de Asuntos Exteriores y de Cooperación–Agencia Española de Cooperación Internacional (AECI).

## References

- [1] Makarewicz P J and Wilkes G L 1979 *J. Appl. Polym. Sci.* **23** 1619
- [2] Abis A, Braglia R, Camurati I, Merlo E, Natarajan K M, Elwood D *et al* 1994 *J. Appl. Polym. Sci.* **52** 1431
- [3] Habibelahi M, Ehsani M and Morshedian J 2019 *Polyolefins J.* **6** 75
- [4] Zhang G Y, Ma J W, Cui B X, Luo X L and Ma D Z 2001 *Macromol. Chem. Phys.* **202** 604
- [5] Meziane O, Guessoum M, Bensedira A and Haddaoui N 2017 *J. Polym. Eng.* **37** 577
- [6] Murff S R, Barlow J W and Paul D R 1984 *J. Appl. Polym. Sci.* **29** 3231
- [7] Ishigami A, Kodama Y, Wagatsuma T and Ito H 2017 *Int. Polym. Process.* **32** 568
- [8] da Silva G A M, Barcelos K A, Coelho da Silva M and Morelli C L 2020 *Polym. Polym. Compos.* **28** 331
- [9] Garcia M, Eguiazabal J I and Nazabal J 2001 *J. Appl. Polym. Sci.* **81** 121
- [10] Dal Lago E, Boaretti C, Piovesan F, Roso M, Lorenzetti A and Modesti M 2018 *Materials* **12** 49
- [11] Al-Jabareen A, Illescas S, MasPOCH M L I and Santana O O 2010 *J. Mater. Sci.* **45** 2907
- [12] Al-Jabareen A, Illescas S, MasPOCH M L I and Santana O O 2010 *J. Mater. Sci.* **45** 6623
- [13] Carrot C, Mbarek S, Jaziri M and Chalamet Y 2007 *Macromol. Mater. Eng.* **292** 693
- [14] Nabar S and Kale D D 2007 *J. Appl. Polym. Sci.* **104** 2039
- [15] Mendes L C, Pereira P S C and Ramos V D 2011 *Macromol. Symp.* **299** 183
- [16] Pereira P S C, Mendes L C and Ramos V D 2010 *Macromol. Symp.* **290** 121
- [17] Mendes L C, Pereira P S C, Abrigo R E R and Ramos V D J 2010 *J. Therm. Anal. Calorim.* **99** 545
- [18] Pereira P S C, Mendes L C and Abrigo R E R 2008 *Int. J. Polym. Mater.* **57** 494
- [19] Maruhashi Y and Iida S 2001 *Polym. Eng. Sci.* **41** 1987
- [20] Billmeyer F W 1966 *Mater. Res. Stand.* **6** 295
- [21] Pilati F, Marianucci E and Berti C 1985 *J. Appl. Polym. Sci.* **30** 1267
- [22] Dealy J M and Wissbrun K F 1999 *Melt rheology and its role in plastics processing: theory and applications* (The Netherlands: Kluwer Academic Publishers)
- [23] Ignatov V N, Carraro C, Tartari V, Pippa R, Scapin M, Pilati F *et al* 1997 *Polymer* **38** 201
- [24] Ignatov V N, Carraro C, Tartari V, Pippa R, Scapin M, Pilati F *et al* 1997 *Polymer* **38** 195
- [25] Ignatov V N, Carraro C, Tartari V, Pippa R, Scapin M, Pilati F *et al* 1996 *Polymer* **37** 5883
- [26] van Gurp M and Palmen J 1998 *Rheol. Bull.* **67** 5
- [27] Trinkle S and Friedrich C 2001 *Rheol. Acta* **40** 322
- [28] Fleury G, Schlatter G and Muller R 2004 *Rheol. Acta* **44** 174
- [29] Choi S J and Showalter W R 1995 *Phys. Fluids* **33** 420
- [30] Gleinser W, Braun H, Friedrich C, and Cantow J 1994 *Polymer* **35** 128
- [31] Macaúbas P H P and Demarquette N R 2001 *Polymer* **42** 2543
- [32] Lacroix C, Bousmina M, Carreau P J, Favis B D and Michel A 1996 *Polymer* **37** 2939
- [33] Lacroix C, Aressy M and Carreau P J 1997 *Rheol. Acta* **36** 416
- [34] Huitric J, Médéric P, Moan M and Jarrin J 1998 *Polymer* **39** 4849
- [35] Gross B 1953 *Mathematical structure of the theories of viscoelasticity* (Paris, France: Hermann et Cie)
- [36] Wu S 1987 *Polym. Eng. Sci.* **27** 335
- [37] Graebbling D, Muller R and Paliarne J F 1993 *Macromolecules* **26** 320
- [38] Choi S J and Showalter W R 1975 *Phys. Fluids* **18** 420
- [39] Bousmina M and Muller R 1993 *J. Rheol.* **37** 663
- [40] Jeon H S, Nakatani A I, Han C C and Colby R H 2000 *Macromolecules* **33** 9732
- [41] Coran A Y and Patel R 1980 *Rubber Chem. Technol.* **53** 141
- [42] Guerrica-Echevarria G, Eguiazabal J I and Nazabal I 2000 *Polym. Test* **19** 849

Springer Nature or its licensor (e.g. a society or other partner) holds exclusive rights to this article under a publishing agreement with the author(s) or other rightsholder(s); author self-archiving of the accepted manuscript version of this article is solely governed by the terms of such publishing agreement and applicable law.